



## Non-Uniform Simple Shear Extrusion (NUSSE) Technique as a novel sever plastic deformation technique

Ali Izi, Mohammad Honarpisheh\*, Farshid Ahmadi

Faculty of Mechanical Engineering, University of Kashan, Kashan, Iran.

Received: 10 January 2024; Accepted: 26 April 2024

\*Corresponding author email: [honarpisheh@kashanu.ac.ir](mailto:honarpisheh@kashanu.ac.ir)

### ABSTRACT

In this research, a new technique for severe plastic deformation (SPD) was proposed, entitled as non-uniform simple shear extrusion (NUSSE). The larger strains can be obtained in the non-uniform simple shear extrusion (NUSSE) method without repetition of the process. But, in pure shear extrusion (PSE) and simple shear extrusion (SSE) processes, to achieve larger strains, it is necessary to repeat the processes. In this study, the technique was investigated experimentally and numerically using ABAQUS software. The maximum plastic strain, inhomogeneity in deformation, filling fraction and micro-hardness parameters were researched after NUSSE process. Also, the obtained results were compared to the SSE and PSE processes. After this technique, due to the specific design of deformation channel, filling fraction was increased by about 44.92% and 41.84% in comparison with SSE and PSE processes, respectively. Also, the micro-hardness was significantly increased compared to annealing process.

**Keywords** Sever plastic deformation, Non-Uniform Simple Shear Extrusion, Filling fraction, Inhomogeneity in deformation, Micro-hardness.

### 1. Introduction

Sever plastic deformation (SPD) processes are known as powerful tools for improving the mechanical properties of metals [1]. In this regard, nowadays, the issue of improving SPD techniques is a wish of many researchers [2-3]. Some of the most-used SPD techniques include Equal-channel angular pressing (ECAP) [4], Non-equal channel angular pressing (NECAP) [5-6], Tubular channel angular pressing (TCAP) [7], Cyclic close die forging (CCDF) [8-9-10], High-pressure torsion (HPT) [11], Pure shear extrusion (PSE) [12], Twist extrusion (TE) [13], Simple shear extrusion (SSE) [14], Constrained groove pressing (CGP) [15-16] and Equal-channel angular rolling (ECAR) [17-18]. However, in recent years, the SSE method has the

most development compared to other SPD methods. But one of the disadvantages of this technique is necessity to repeat the method to achieve larger strains [19-20]. Ebrahimi et al. [14] introduced the SSE technique for first time experimentally and by numerical simulation. They showed in the SSE process, due to the special design of the die channel and gradual changes in the cross-sectional area of the sample, large strain values can be obtained for aluminum alloy 1050 by SSE process. Also, investigated the effect of the amount of back pressure on the strain value and the final shape of the samples after the SSE process, they reported that the both parameters are dependent on the amount of back pressure. Also, they presented that the SSEed samples have less amount of waste material in compari-

son with ECAPed samples. Pardis et al. [21] investigated the effect of different processing routes (four routes A-D) on the homogeneity of deformation in the SSE technique for aluminum alloy 1050. They presented that in the route C, since the sample has a 90° rotation around its main axis, the homogeneity of deformation is obtained more than route B. Bayat Tork et al. [22] investigated the effect of SSE process on the feasibility of plastic deformation of pure magnesium at room temperature. They showed that in the ECAP, channel angular deformation (CAD) and dual equal channel lateral extrusion (DECLLE) processes, due to the samples have the high level of segmentation, so the SSE method is suitable for producing and improving the microstructure of pure magnesium at the room temperature compared to the mentioned processes. Bagherpour et al. [23] studied on the capability of processing twinning induced plasticity (TWIP) steel through SSE and ECAP processes. They concluded that in the ECAP process, due to the existence of segmentation flow during the ECAP process after one pass,

the SSE process can be the ideal choice for processing TWIP steel. Ebrahimi et al. [24, 25] introduced the new design of SSE process for producing samples of aluminum alloy 1050, called circular simple shear extrusion (CSSE). They showed in the CSSE method, due to the circular cross section of the die channel, the extrusion pressure, the load required for deformation, the maximum principle stress and the amount of back pressure for fill the die channel are less in comparison with SSE method. Also, they reported that the CSSE method is more useful for producing industrial parts because the circular cross section is a suitable shape for most industrial parts. Rezvani et al [26] investigated the effect of CSSE process on deformation behavior and strain distribution of commercially pure aluminum. After experimental and simulation tests, they showed that the most homogeneity distribution of strain is obtained in the cross section and the length of the specimens without back pressure. The CSSE process had a significant effect on increasing the micro-hardness compared to the annealing process.

Table 1- Chemical composition of AA1050 aluminum alloy (wt %)

| Element | Si   | Fe  | Cu   | Mn   | Mg   | Zn   | Ti   | V    | Each other | Al      |
|---------|------|-----|------|------|------|------|------|------|------------|---------|
| Wt %    | 0.25 | 0.4 | 0.05 | 0.05 | 0.05 | 0.05 | 0.03 | 0.05 | 0.03       | Balance |

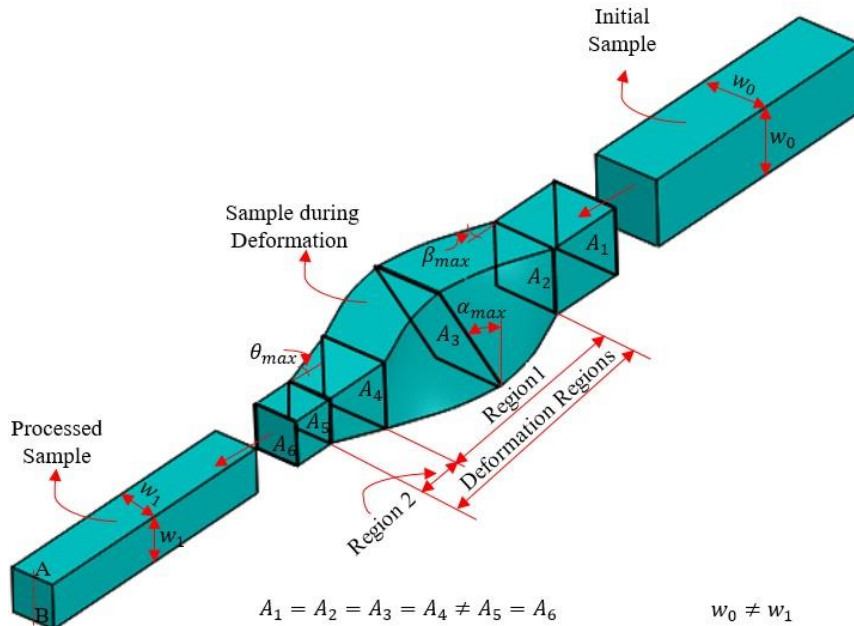


Fig. 1- a schematic of the NUSSE technique, geometry of the deformation channel and gradual changes of the specimen's cross section through the die channel.

Also, with the increase in the number of passes, the grains size was greatly reduced.

In this study, the non-uniform simple shear extrusion (NUSSE) method is introduced as a new SPD technique for the first time. After this process, larger strains can be achieved without repeating the method. The method can be very easily installed on any standard industrial and laboratory equipment. These can be important advantages of this technique. The technique was investigated experimentally and numerically using ABAQUS/Explicit on AA1050 alloy. The effect of the NUSSE was studied on strain plastic, filling fraction, inhomogeneity in deformation and micro-hardness specimen. Also, they were compared to SSE and PSE processes.

## 2. NUSSE Process

In this method, the samples were extruded gradually through a deformation channel with a specific design (Fig. 1). Fig. 1 shows, a schematic of the samples position in the NUSSE process, geometry of the deformation channel and the sample's cross section changes during the NUSSE process. In this

figure,  $w_0$ ,  $w_1$ ,  $\alpha_{max}$ ,  $\beta_{max}$ , and  $\theta_{max}$  are the inlet channel thickness, the outlet channel thickness, maximum distortion angle, maximum inclination angle and maximum angle of region 2, respectively. Also,  $A_1$  and  $A_6$  are the cross-section of input channel and output channel, respectively.

## 3. Experimental Procedure

Billets with dimensions of 15 mm × 15 mm × 60 mm were machined out from rolled plate of aluminum AA1050. Chemical composition of the plate is shown in Table 1. The specimens were annealed at 600 °C for 2 h [14] and cooled to ambient temperature in furnace. In the study, these annealed specimens are called the initial specimens.

The experimental tests were carried out at ambient temperature using a 100 Ton hydraulic press machine with ram speed of 0.05mm s<sup>-1</sup>. Fig. 2a indicates the equipment needed to perform the process. In the designed die,  $w_0$ ,  $w_1$ ,  $\alpha_{max}$ ,  $\beta_{max}$ ,  $2\theta_{max}$  were 15 mm, 10 mm, 45°, 22.2° and 30°, respectively (Fig. 1b). In order to reduce friction between the sample and the die channel, after the samples

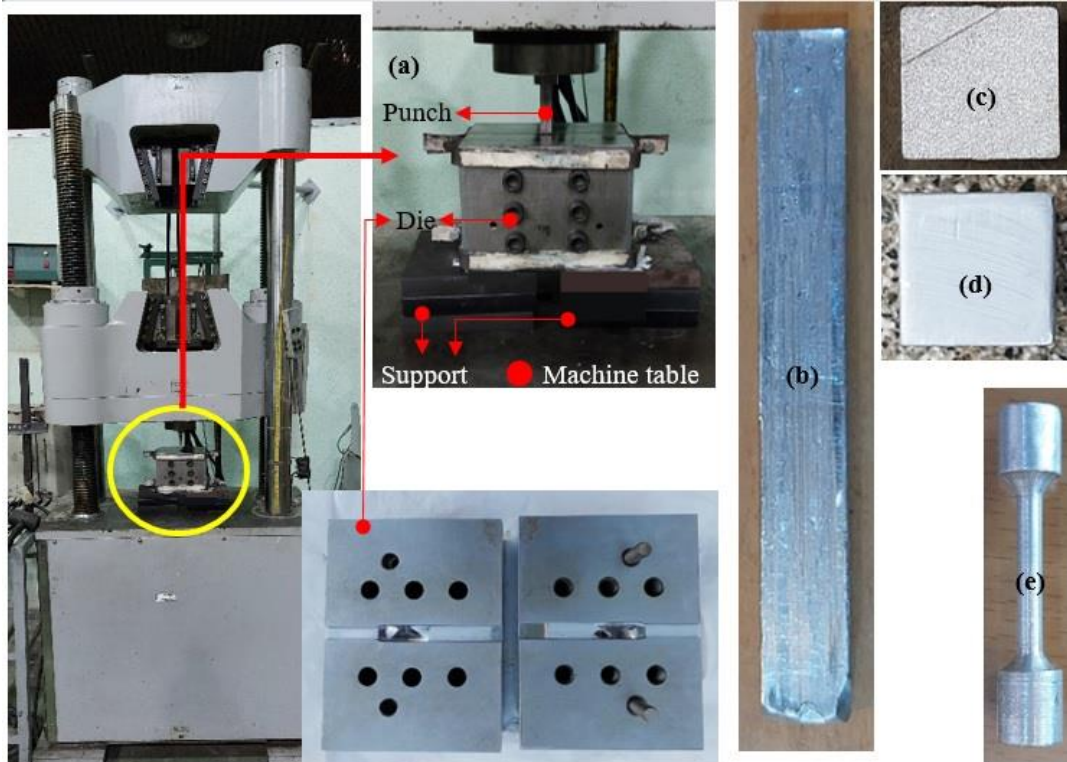


Fig. 2- a schematic set-up the NUSSE method, b NUSSEed specimen, c Specimen's cross section of the NUSSEed specimen obtained experimentally, d Specimen's cross section before NUSSE and e Tensile test specimen.

were wrapped with Teflon tape, MoS<sub>2</sub> anti-friction spray was used as lubrication. In Fig. 2b, c and d, the NUSSEd sample, the cross-sectional area of the NUSSEd and annealed samples, obtained experimentally is shown, respectively.

According to the ASTM B557M standard, the annealed sample was machined for done tensile test (Fig. 2e). This test was performed at the ambient temperature with the strain rate of 10<sup>-3</sup> s<sup>-1</sup>. Fig. 3 indicates engineering stress-strain curve achieved from the tensile test for the annealed sample.

In the study, the Vickers micro-hardness tester was used to measure the hardness of NUSSEd and annealed samples. The samples were isolated into two equal sections using the wire cut method. The hardness values were taken on one of the cutting surfaces under conditions of 25 g load for 15s. The distance between the measuring points on the line AB for both samples was 0.5 mm.

#### 4. Simulation Procedure

In this study, the deformation processes were investigated numerically by the ABAQUS/Explicit 6.14 package. The 3D FEM was performed to check the strain homogeneity, the maximum equivalent plastic strain and filling fraction in the different techniques. The finite element assembly model of the die, the punch and sample in the NUSSE technique is illustrated in Fig. 4. The sample was considered as an elasto-plastic material with Young's modulus and Poisson ratio of 70 GPa and 0.33, respectively. The die and the punch were considered

as rigid bodies. The uniaxial tensile test was done to obtain the sample properties. In the study, the punch speed was equal to 0.05 mm s<sup>-1</sup>. This value was constant in all experimental and numerical tests. The interaction between the punch and die channel surfaces with the specimen surfaces was defined based on the Coulomb's frictional model. Friction factor (*m*) of 0 and 0.1 were used. These values in simulation were converted to friction coefficient ( $\mu$ ) by Eq. (1) [27]. In this paper, 108000 C3D8R elements was used for the sample, 22446 and 306 R3D4 rigid elements were employed for the die and the punch, respectively.

$$\mu = \frac{m}{\sqrt{27(1 - m^2)}} \quad (1)$$

#### 4.1. Filling fraction (*F<sub>f</sub>*)

Filling fraction is calculated by using the following relation:

$$F_f = \frac{S_s}{S_c} \times 100 \quad (2)$$

Where *S<sub>s</sub>* is the cross-sectional area of the specimen after deformation, and *S<sub>c</sub>* is the cross-sectional area of the die outlet channel at extrusion direction.

#### 4.2. Standard Deviation (S. D)

In this study, the standard deviation (S. D) is used to investigate the effect of deformation processes on strain homogeneity. This criterion was measured based on the strain distribution along

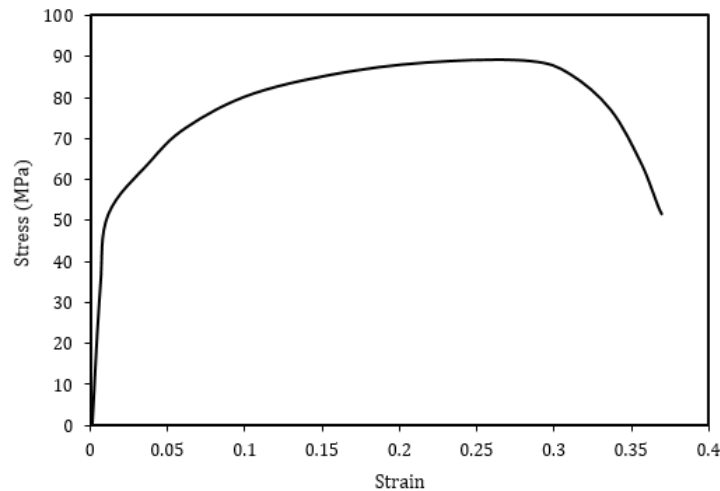


Fig. 3- Engineering stress-strain curve achieved from the tensile test for the annealed sample.

line AB of the sample's cross section. Standard deviation is calculated using Eq. (3) [28]:

$$S.D = \sqrt{\frac{\sum_{i=1}^N (\varepsilon_i - \varepsilon_{avg})^2}{N - 1}} \quad (3)$$

Where  $\varepsilon_i$ ,  $\varepsilon_{avg}$  and N are the effective strain for the  $i$ th point, the average effective strain and the number of the measurement points, respectively. The lower value S.D means more homogeneity in the strain.

## 5. Results and Discussion

### 5.1. Filling Fraction

In Fig. 1, gradual changes of the cross-sectional area of the sample through the deformation channel in the NUSSE process is shown. Fig. 5 illustrates the cross-sectional area of the specimen at the die outlet channel on a perpendicular plane to the extrusion direction which is obtained experimentally and numerically after the NUSSE process. It is observed that the specimen has fully filled in die exit channel and gaps are not formed at the cor-

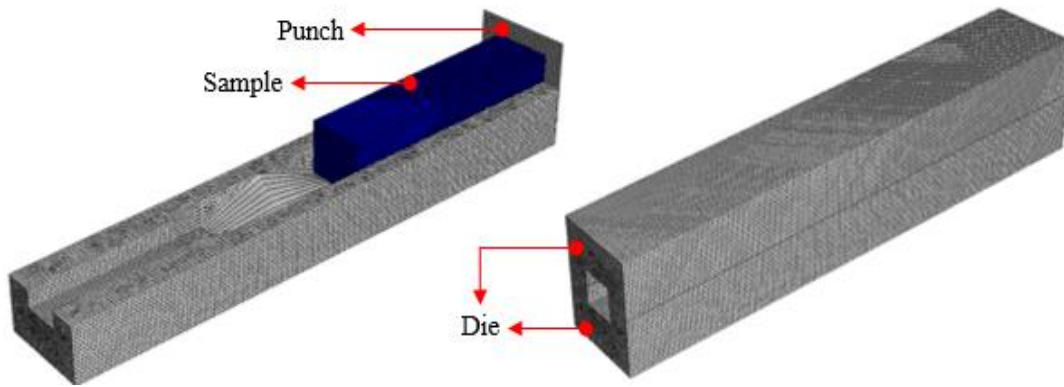


Fig. 4- 3D FEM model of the sample, the die, and the punch for the NUSSE process simulation.

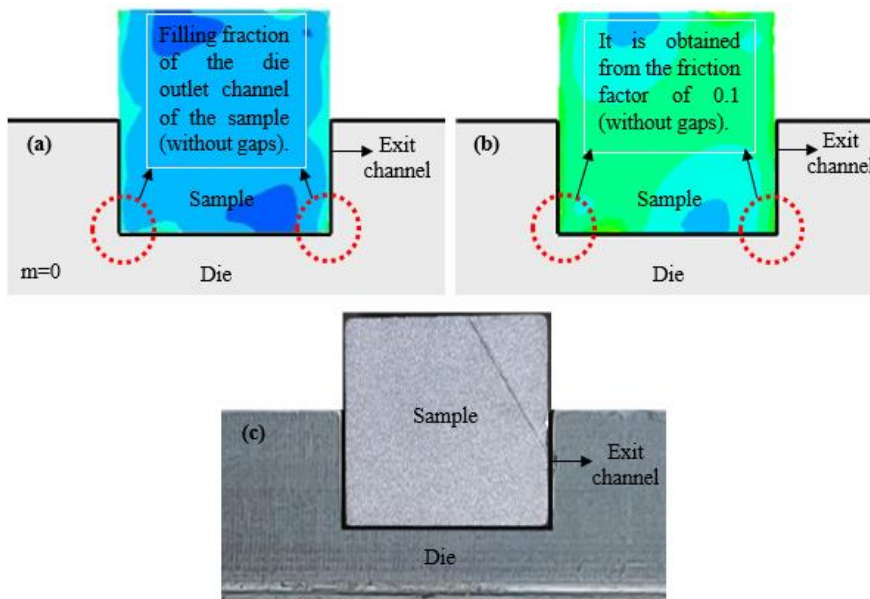


Fig. 5- schematic sample's cross section obtained by simulation a form the friction factor of 0, b from the friction factor of 0.1 and c sample's cross section obtained experimentally.

ners of the sample. It shows that the NUSSE process provides ideal conditions for the deformation sample. In order the specimen is totally returned to the die channel shape. Similar results have been reported: for ECAP [28] and PSE [29] processes. Also, it shows that there is a good agreement between the final cross section of the simulated and the experimental sample (Fig. 5). In Fig. 8, the effect of friction factor ( $m$ ) and the processing conditions on the filling fraction of the die outlet channel, obtained using the Eq. (2) is shown. It is clear that due to the specific shape of the die channel, the friction factor value has not the significant effect on the filling fraction in this technique. Therefore, the  $F_f$  increases by about 44.92% and 41.84% in comparison to SSE and PSE processes, respectively (Fig. 5). According to Fig. 5, the sample's cross section is completely regular after this method. Therefore, it

is an important advantage of NUSSE technique in comparison with SSE and PSE processes (Figs. 6b and 7b).

Also, to comparison with the NUSSE process, the inhomogeneity of strain, the maximum equivalent plastic strain  $\epsilon_{pmax}^e$  and filling fraction  $F_f$  parameters were obtained numerically in the SSE process after first pass with  $\alpha_{max}=45^\circ$  and  $\beta_{max}=22.2^\circ$ . The processing conditions ( $m=0.1$ , punch speed and etc) and mechanical properties were same in both processes, the die was designed based on samples with dimensions of  $10 \times 10 \times 60$  mm. Fig. 6a and b shows the schematic of the 3D FEM model of the SSE process and sample's cross section after the SSE, respectively. Fig. 8 indicates that  $F_f$  value decreases after SSE process and this value is by about 31% smaller than the NUSSE process.

Also, to comparison with NUSSE technique, the

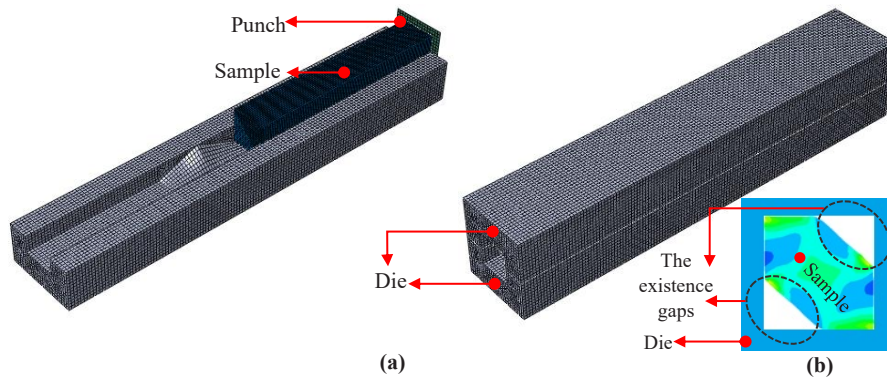


Fig. 6- Schematic a 3D FEM model of the SSE process simulation and b the cross sectional of the SSEed sample.

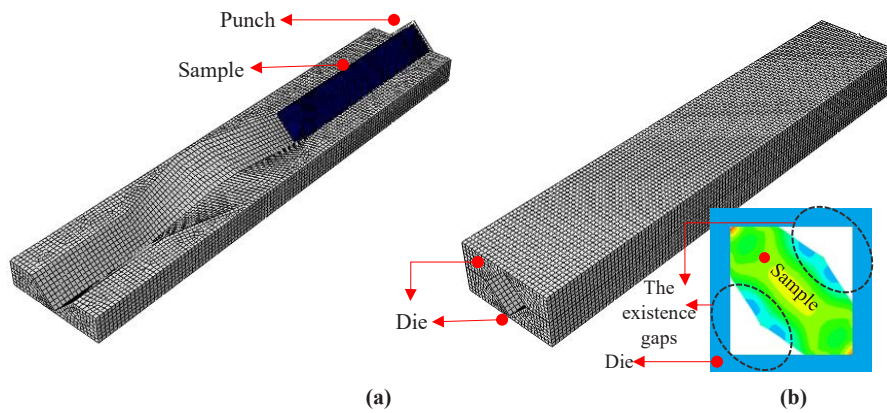


Fig. 8- Schematic a 3D FE model of the PSE process simulation and b the cross sectional of the PSEed sample.

S.D,  $\epsilon_{pmax}^e$  and  $F_f$  parameters were achieved numerically in the PSE after first pass with  $L_{DZI}=50$  mm,  $L_{RZ}=10$  mm and  $D_R=2$ . The mechanical properties and the processing conditions ( $m=0.1$ , punch speed and etc) were constant for both processes, the die channel was designed based on specimens with dimensions of  $10 \times 10 \times 60$  mm. Fig. 7a and b illustrates the schematic of the 3D FEM model of the PSE process and sample's cross section obtained

numerically, respectively. According to Fig. 8, it is observed that the amount of  $F_f$  is significantly lower for the PESeD sample than NUSSEd sample.

**5.2. Plastic Strain**

Fig. 9 illustrates the distribution 2D of equivalent plastic strain in the cross-sectional area of the sample, obtained numerically, for different processes under the same conditions ( $m=0.1$ ). In Fig. 10a and

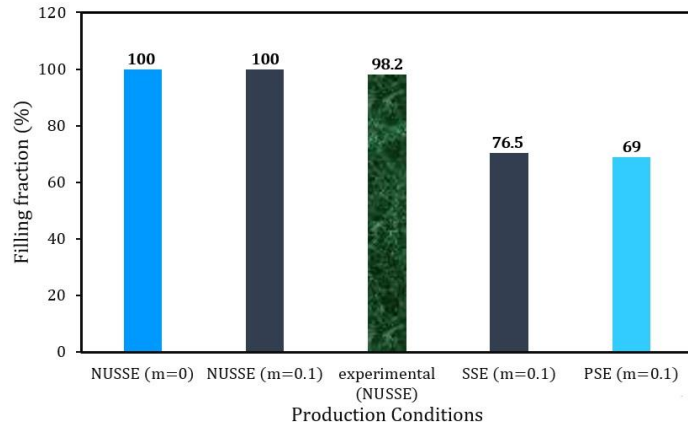


Fig. 8- The effect of friction factor (m) and the processing conditions on the filling fraction ( $F_f$ ) of the die outlet channel obtained by the Eq. (2).

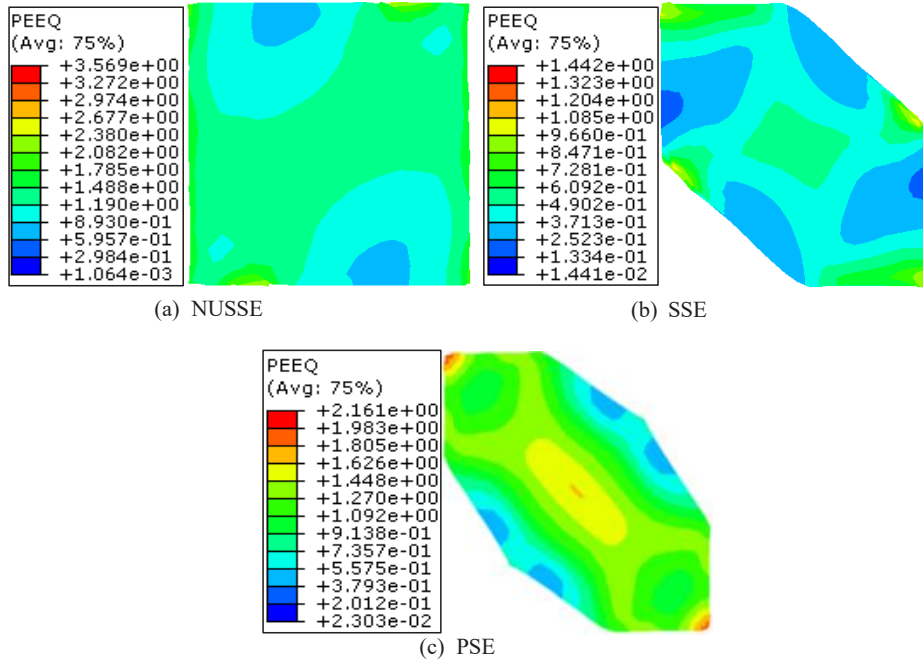


Fig. 9- Distribution 2D of the  $\epsilon_p^e$  a in the NUSSEd sample, b in the SSEd sample and c in the PSEd sample, are obtained by the FEM, from the friction factor of 0.1.

b, the effective strain distribution along line AB and the maximum effective strain, are obtained from the FEM, for different samples, from the friction factor of 0.1 is shown, respectively. It is observed that the maximum strain is achieved in the center regions of the samples (Fig. 10a). According to Fig. 12, due to strain hardening, the hardness increases

es in the sample center. Therefore, with increasing hardness, plastic strain is affected by it. It can be stated that the center regions experience more strain compared to the peripheral regions. Also, due to the special shape of the NUSSE die channel, this technique produces larger strains than SSE and PSE processes (Fig. 10a). It can be expressed as a

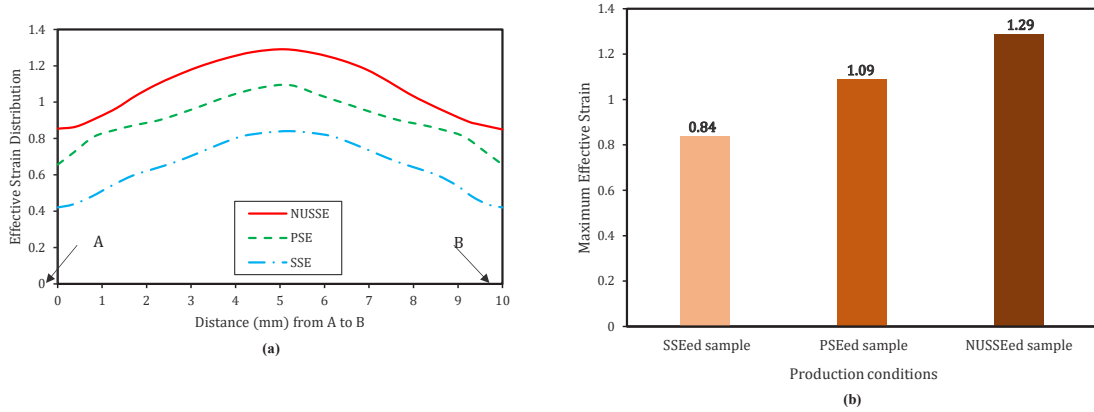


Fig. 10- A distribution of effective strain along line AB, and b the maximum effective strain, are obtained from the FEM, for different processes, from the friction factor of 0.1.

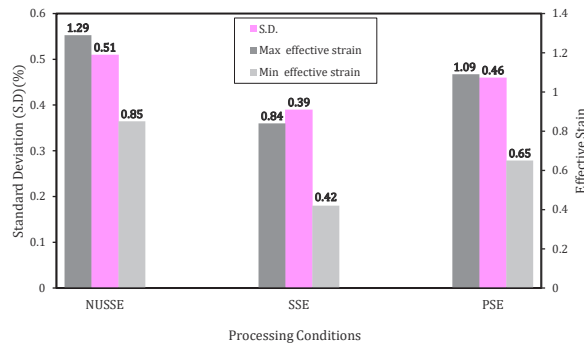


Fig. 11- Inhomogeneity of strain obtained from Eq. (3), for the samples with different processing conditions, from  $m=0.1$ .

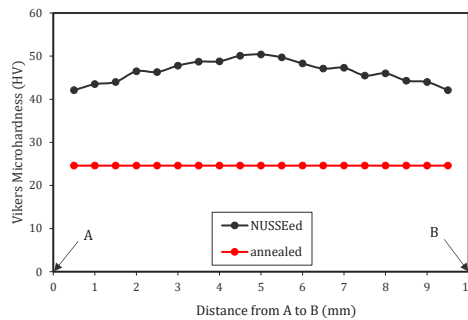


Fig. 12- Hardness profiles obtained from the Vickers test along line AB for samples processed under different conditions.

major advantage of the NUSSE process.

### 5.3. Inhomogeneity of Strain

Fig. 11 indicates the inhomogeneity of strain, obtained by numerical simulation, from  $m=0.1$ , for the different samples. In Fig. 11, standard deviation (S. D) is calculated by the Eq. (3) for 21 points. It is observed that the S. D is increased after NUSSE process. Therefore, with the increase of S. D, uniformity of deformation is reduced compared to SSE and PSE processes (Fig. 12). Due to the existence of different deformation regions, the gradual imposition of sample deformation during the NUSSE process and creating great deformations, they can be expressed as the reason for the increase of S. D in this technique. Similar results have been reported: for SSE [21], ECAP [28] and PSE [29-32] processes.

### 5.4. Hardness Measurement

Fig. 12 indicates the hardness profile obtained from the Vickers micro-hardness test along line AB for different samples. It is observed that the annealed and NUSSEd samples have the maximum hardness by about 24.6 HV (red line) and 50.6 HV (black line), respectively. Therefore, NUSSE process has the considerably effect on the hardness in comparison with anneal process. Similar results have been reported: for SSE [14], CSSE [26], PSE [29], and TE [33] processes.

## 6. Conclusion

In this study, NUSSE was introduced as a new

SPD method. The technique was investigated experimentally and numerically on AA1050 alloy. The process simulation was carried out with the help of ABAQUS/Explicit 6.14. Moreover, the filling fraction, maximum plastic Strain, effective strain distribution, inhomogeneity of strain and micro-hardness parameters were studied. Also, the obtained results were compared with SSE and PSE processes. The main obtained results of this paper could be summarized as follows:

1. Due to the special shape of the die channel in the NUSSE process, the process has the necessary ability to produce bulk materials with larger strains and regular cross section without repeating the process.

2. The obtained results show that the fraction factor has not the significant effect on the filling fraction in this technique. Also, filling fraction increases by about 44.92% and 41.84% in comparison with SSE and PSE processes, respectively.

3. After performing the NUSSE technique, the Vickers micro-hardness increases by about 87.93% in comparison with annealed sample. Also, the maximum effective strain increases by about 53.57% and 18.34% in comparison with SSE and PSE processes, respectively.

4. Due to the existence of different deformation regions, the gradual imposition of sample deformation during the NUSSE process and creating great deformations, the strain homogeneity decreases by about 23.53% and 9.8% in comparison with SSE and PSE processes, respectively.

## References

1. Bayat Tork N, Saghafian H, Razavi SH, Al-Fadhalah KJ, Ebrahimi R, Mahmudi R. Microstructure and texture characterization of Mg-Al and Mg-Gd binary alloys processed by simple shear extrusion. *Journal of Materials Research and Technology*. 2019;8(1):1288-99.
2. Horita Z. *Nanomaterials by Severe Plastic Deformation*. Materials Science Forum: Trans Tech Publications Ltd; 2006.
3. Valiev RZ, Estrin Y, Horita Z, Langdon TG, Zechetbauer MJ, Zhu YT. Producing bulk ultrafine-grained materials by severe plastic deformation. *JOM*. 2006;58(4):33-9.
4. Azushima A, Kopp R, Korhonen A, Yang DY, Micari F, Lahoti GD, et al. Severe plastic deformation (SPD) processes for metals. *CIRP Annals*. 2008;57(2):716-35.
5. Khanlari H, Honarpisheh M. An upper bound analysis of channel angular pressing process considering die geometric characteristics, friction, and material strain-hardening. *CIRP Journal of Manufacturing Science and Technology*. 2023;41:259-76.
6. Khanlari H, Honarpisheh M. Investigation of Microstructure, Mechanical Properties and Residual Stress in Non-equal-Channel Angular Pressing of 6061 Aluminum Alloy. *Transactions of the Indian Institute of Metals*. 2020;73(5):1109-21.
7. Aghababaei A, Honarpisheh M. Experimental and numerical investigation of residual stress distribution in Al-6061 tubes under using tubular channel angular pressing process by new trapezoidal channel. *The Journal of Strain Analysis for Engineering Design*. 2022;58(4):332-42.
8. Moazam MA, Honarpisheh M. Improving the mechanical properties and reducing the residual stresses of AA7075 by combination of cyclic close die forging and precipitation hardening. *Proceedings of the Institution of Mechanical Engineers, Part L: Journal of Materials: Design and Applications*. 2020;235(3):542-9.
9. Moazam MA, Honarpisheh M. The effects of combined cyclic close die forging and aging process on microstructure and mechanical properties of AA7075. *Proceedings of the Institution of Mechanical Engineers, Part L: Journal of Materials: Design and Applications*. 2020;234(9):1242-51.
10. Moazam MA, Honarpisheh M. Ring-core integral method to measurement residual stress distribution of Al-7075 alloy processed by cyclic close die forging. *Materials Research Express*. 2019;6(8):0865j3.
11. Zhilyaev AP, Langdon TG. Using high-pressure torsion for metal processing: Fundamentals and applications. *Progress in Materials Science*. 2008;53(6):893-979.

12. Eivani AR, Rahimi F. Inhomogeneity in deformation, microstructure, tensile properties and damage development in AA1050 during multiple cycles of pure shear extrusion. *Materials Science and Engineering: A*. 2019;745:159-67.
13. Beygelzimer Y, Varyukhin V, Synkov S, Orlov D. Useful properties of twist extrusion. *Materials Science and Engineering: A*. 2009;503(1-2):14-7.
14. Pardis N, Ebrahimi R. Deformation behavior in Simple Shear Extrusion (SSE) as a new severe plastic deformation technique. *Materials Science and Engineering: A*. 2009;527(1-2):355-60.
15. Nazari F, Honarpisheh M. Analytical model to estimate force of constrained groove pressing process. *Journal of Manufacturing Processes*. 2018;32:11-9.
16. Nazari F, Honarpisheh M, Zhao H. Effect of stress relief annealing on microstructure, mechanical properties, and residual stress of a copper sheet in the constrained groove pressing process. *The International Journal of Advanced Manufacturing Technology*. 2019;102(9-12):4361-70.
17. Kotobi M, Honarpisheh M. Uncertainty analysis of residual stresses measured by slitting method in equal-channel angular rolled Al-1060 strips. *The Journal of Strain Analysis for Engineering Design*. 2016;52(2):83-92.
18. Honarpisheh M, Haghighat E, Kotobi M. Investigation of residual stress and mechanical properties of equal channel angular rolled St12 strips. *Proceedings of the Institution of Mechanical Engineers, Part L: Journal of Materials: Design and Applications*. 2016;232(10):841-51.
19. Bagherpour E, Qods F, Ebrahimi R, Miyamoto H. Strain reversal in simple shear extrusion (SSE) processing: Microstructure investigations and mechanical properties. *AIP Conference Proceedings*: Author(s); 2018.
20. Sedehi SMR, Khosravi M, Yaghoobinezhad Y. Mechanical properties and microstructures of reduced graphene oxide reinforced titanium matrix composites produced by spark plasma sintering and simple shear extrusion. *Ceramics International*. 2021;47(23):33180-90.
21. Pardis N, Ebrahimi R. Different processing routes for deformation via simple shear extrusion (SSE). *Materials Science and Engineering: A*. 2010;527(23):6153-6.
22. Tork NB, Pardis N, Ebrahimi R. Investigation on the feasibility of room temperature plastic deformation of pure magnesium by simple shear extrusion process. *Materials Science and Engineering: A*. 2013;560:34-9.
23. Bagherpour E, Reihanian M, Ebrahimi R. On the capability of severe plastic deformation of twinning induced plasticity (TWIP) steel. *Materials & Design (1980-2015)*. 2012;36:391-5.
24. Ebrahimi R, Rezvani A, Bagherpour E. Circular simple shear extrusion as an alternative for simple shear extrusion technique for producing bulk nanostructured materials. *Procedia Manufacturing*. 2018;15:1502-8.
25. Rezvani A, Bagherpour E, Ebrahimi R. Circular Simple Shear Extrusion as an Alternative to Simple Shear Extrusion Technique. *Iranian Journal of Science and Technology, Transactions of Mechanical Engineering*. 2018;44(1):193-201.
26. Rezvani A., Ebrahimi, R. Investigation on the Deformation Behavior and Strain Distribution of Commercially Pure Aluminum after Circular Simple Shear Extrusion. *Journal of Ultrafine Grained and Nanostructured Materials*, 2019; 52(1): 32-42.
27. Bay N. Friction stress and normal stress in bulk metal-forming processes. *Journal of Mechanical Working Technology*. 1987;14(2):203-23.
28. Djevanroodi F, Daneshlab M, Ebrahimi M. A novel technique to increase strain distribution homogeneity for ECAPed materials. *Materials Science and Engineering: A*. 2012;535:115-21.
29. Rahimi F, Eivani AR, Kiani M. Effect of die design parameters on the deformation behavior in pure shear extrusion. *Materials & Design*. 2015;83:144-53.
30. Bagherpour E, Qods F, Ebrahimi R. Effect of geometric parameters on deformation behavior of simple shear extrusion. *IOP Conference Series: Materials Science and Engineering*. 2014;63:012046.
31. Sedehi SMR, Khosravi M, Yaghoobinezhad Y. Mechanical properties and microstructures of reduced graphene oxide reinforced titanium matrix composites produced by spark plasma sintering and simple shear extrusion. *Ceramics International*. 2021;47(23):33180-90.
32. Rahimi F, Eivani AR. A new severe plastic deformation technique based on pure shear. *Materials Science and Engineering: A*. 2015;626:423-31.
33. Bagherpour E, Reihanian M, Ebrahimi R. Processing twinning induced plasticity steel through simple shear extrusion. *Materials & Design*. 2012;40:262-7.